REGULAR ARTICLE

blood advances

CAR19 monitoring by peripheral blood immunophenotyping reveals histology-specific expansion and toxicity

Mark P. Hamilton,[1-3] Erin Craig,[4] Cesar Gentille Sanchez,[1] Alain Mina,[1] John Tamaresis,[4] Nadia Kirmani,[1] Zachary Ehlinger,[1] Shriya Syal,[1] Zinaida Good,[1,4] Brian Sworder,[3] Joseph Schroers-Martin,[3] Ying Lu,[4] Lori Muffly,[1,2] Robert S. Negrin,[1,2] Sally Arai,[1,2] Robert Lowsky,[1,2] Everett Meyer,[1,2] Andrew R. Rezvani,[1,2] Judith Shizuru,[1,2] Wen-Kai Weng,[1,2] Parveen Shiraz,[1,2] Surbhi Sidana,[1,2] Sushma Bharadwaj,[1,2] Melody Smith,[1,2] Saurabh Dahiya,[1,2] Bita Sahaf,[1] David M. Kurtz,[3] Crystal L. Mackall,[1,2] Robert Tibshirani,[4] Ash A. Alizadeh,[3,5,6,*] Matthew J. Frank,[1,2,*] and David B. Miklos[1,2,*]

[1]Center for Cancer Cell Therapy, Stanford Cancer Institute, [2]Division of Blood and Marrow Transplantation and Cellular Therapy, Department of Medicine, [3]Division of Oncology, Department of Medicine, and [4]Department of Biomedical Data Science, Stanford University School of Medicine, Stanford, CA, [5]Institute for Stem Cell Biology and Regenerative Medicine, and [6]Stanford Cancer Institute, Stanford University, Stanford, CA

Key Points

- MCL has increased CAR19 expansion and toxicity relative to LBCL or follicular lymphoma.
- CAR19 expansion in LBCL is strongly associated with toxicity but not efficacy.

Chimeric antigen receptor (CAR) T cells directed against CD19 (CAR19) are a revolutionary treatment for B-cell lymphomas (BCLs). CAR19 cell expansion is necessary for CAR19 function but is also associated with toxicity. To define the impact of CAR19 expansion on patient outcomes, we prospectively followed a cohort of 236 patients treated with CAR19 (brexucabtagene autoleucel or axicabtagene ciloleucel) for mantle cell lymphoma (MCL), follicular lymphoma, and large BCL (LBCL) over the course of 5 years and obtained CAR19 expansion data using peripheral blood immunophenotyping for 188 of these patients. CAR19 expansion was higher in patients with MCL than other lymphoma histologic subtypes. Notably, patients with MCL had increased toxicity and required fourfold higher cumulative steroid doses than patients with LBCL. CAR19 expansion was associated with the development of cytokine release syndrome, immune effector cell–associated neurotoxicity syndrome, and the requirement for granulocyte colony-stimulating factor 14 days after infusion. Younger patients and those with elevated lactate dehydrogenase (LDH) had significantly higher CAR19 expansion. In general, no association between CAR19 expansion and LBCL treatment response was observed. However, when controlling for tumor burden, we found that lower CAR19 expansion in conjunction with low LDH was associated with improved outcomes in LBCL. In sum, this study finds CAR19 expansion principally associates with CAR-related toxicity. Additionally, CAR19 expansion as measured by peripheral blood immunophenotyping may be dispensable to favorable outcomes in LBCL.

Introduction

CD19-directed chimeric antigen receptor (CAR) T-cell (CAR19) therapy has revolutionized the treatment of non-Hodgkin lymphoma. CAR19 is currently approved for second-line treatment of large B-cell lymphoma (LBCL)[1-7] and mantle cell lymphoma (MCL)[8] and third-line treatment of follicular lymphoma

Submitted 11 January 2024; accepted 7 March 2024; prepublished online on *Blood Advances* First Edition 18 March 2024; final version published online 25 June 2024. https://doi.org/10.1182/bloodadvances.2024012637.

*A.A.A., M.J.F., and D.B.M. contributed equally to this study.

The necessary data to reproduce this work along with comprehensive deidentified annotation of the patients studied in this article are included as supplemental Files, which will serve as a community resource. Additional underlying data or code are available upon request.

The full-text version of this article contains a data supplement.

(FL).[9,10] Despite excellent results in disease control, CAR19 therapy is associated with substantial early and late toxicity. Early toxicity includes cytokine release syndrome (CRS), immune effector cell–associated neurotoxicity syndrome (ICANS), and immune effector cell–associated hemophagocytic lymphohistiocytosis-like syndrome.[11] Late toxicity of CAR19 therapy consists of prolonged cytopenia and infection.[12-14]

Although CAR T-cell therapy is increasingly common, the impact of CAR expansion in relation to its role in driving survival and toxicity end points remains poorly defined. Prior studies demonstrate weak associations between expansion measured by quantitative polymerase chain reaction (qPCR) and cell-free DNA (cfDNA) and response rates[1,3,4,15]; however, other studies failed to show an impact of expansion on these end points when using immune phenotyping.[15,16] CAR expansion is more clearly linked to the development of CRS and ICANS.[1,4,16] In addition to CRS and ICANS toxicities, CAR T-cell therapy is associated with prolonged cytopenias, particularly B-cell aplasia, which is likely related to the persistence of CAR itself.[1,3,4,13]

To understand the impact of CAR19 expansion on patient outcomes in the first month after infusion, we prospectively followed 236 patients treated with either axicabtagene ciloleucel (axi-cel) or brexucabtagene autoleucel (brexu-cel) at Stanford. During this time, we monitored CAR19 expansion in 188 of these patients by real-time peripheral blood immune phenotyping (CAR-FACS) on days 7, 14, 21, and 28 (D7, D14, D21, and D28). We found that MCL histology is associated with increased expansion and toxicity relative to LBCL and FL. CAR expansion was associated with all major toxicities of CAR19 therapy but was not associated with improved survival outcomes in LBCL.

Methods

Clinical data collection

All clinical data collection was reviewed by the Stanford Institutional Review Board (IRB), and the protocols were approved before starting collection. Patients were enrolled continuously and followed longitudinally throughout the study period, with infusion dates ranging from January 2018 to July 2022. Patient data were extracted from the electronic medical record typically from standardized patient notes designed to incorporate critical clinical data related to patients treated with CAR19. Time points were prespecified, and clinical laboratory data were taken from predetermined time points (±2 days).

Progression-free survival (PFS) was the primary survival end point for this study. Time to progression (TTP) and overall survival (OS) were also recorded. Response was determined by Lugano criteria.[17] Progression was determined in conjunction with clinical judgment by the primary treating physician and radiographic or pathologic results. Progression was defined as overwhelming clinical, radiologic, or pathologic evidence of progressing lymphoma (typically by Lugano response criteria followed by biopsy of a growing lesion). PFS was defined as progression or death from any cause. TTP was defined as any progression with end points censored at death from other cause or last follow-up. OS was defined as death from any cause. Time of last contact was defined as the last health care interaction documented in the electronic medical record, including documented clinic contact outside of Stanford University Hospital. Ethnicity and race data were obtained according to National Institutes of Health guidelines. All demographics were based on patient self-identification.

CRS (frequency and grade), ICANS (frequency and grade), and the need for granulocyte colony-stimulating factor (G-CSF) 14 days after infusion were selected as toxicity outcomes. CRS and ICANS were defined by the American Society for Transplantation and Cell Therapy (ASTCT) grading criteria.[18] At Stanford, G-CSF is started at D+1 and stopped once the absolute neutrophil count (ANC) reaches 1000 per mL; it is resumed if ANC falls below 1000 per mL.

Patient sample collection and flow cytometry analysis

Patient samples were collected according to protocol on D7 (±2), D14 (±4), D21 (±4), and D28 (±4). Flow cytometry samples were collected in EDTA or heparin-containing tubes and processed immediately as previously described.[16,19] Briefly, peripheral blood mononuclear cells (PBMCs) were obtained from ~8 mL of fresh whole blood and isolated by density gradient centrifugation with Ficoll-Plague Plus (GE Healthcare). PBMCs were stained with fixable Live/Dead Aqua amine-reactive viability stain (Invitrogen; L-34965). Fc receptors were blocked with Human TruStain FcX (BioLegend; 422302) for 5 minutes to prevent nonspecific antibody binding. Cells were then stained at room temperature with a fluorochrome-conjugated antibody panel.[16] Stained and fixed cells were acquired on a 4-laser LSRII flow cytometer (BD Biosciences; blue: 488-nm, violet: 405-nm, red: 640-nm, and green: 532-nm lasers; 21 parameters). CAR is detected with an anti-idiotype antibody directed against FMC63 (DyLight650 mouse anti-mouse FMC63 scFv; clone 136.20.1).[20] A minimum of a million cells were acquired unless limited by the total number of isolated cells. Gating for CD4+ and CD8+ CAR19s among viable CD45+ cell population was performed using Cytobank software. Sample gating was performed by a team of expert technicians who were blinded to the clinical status of individual patients. Absolute CAR19 counts were obtained by multiplying the percentages of CAR19+ cells among the CD14−CD3+ population by the absolute lymphocyte count on the day of sample acquisition. Assay limit of detection was previously calculated as 1 in 10^4 PBMCs.[16]

Statistical analysis

This study includes 236 patients treated with CAR19. Among them, 188 have associated CAR-FACS data. For clinical data analysis not considering CAR-FACS, all 236 patients were included in data analysis. For longitudinal modeling, all 188 patients with CAR-FACS data were included in analysis. For area under the curve (AUC) analysis, only patients with ≥3 data points over their treatment course were included (124 with LBCL, 19 FL, and 17 MCL). For survival analysis, the 124 patients with LBCL with AUC data were included. For day-specific CAR expansion analysis, all patients with data points available on the respective day were included.

Statistical analysis was performed in R under guidance from the Stanford Department for Biomedical Data Science. Linear mixed effects modeling of longitudinal data was performed using the lme4 package[21] in R with analysis of variance, and *t* tests were performed using the lmerTest package.[22] Multivariate parameters

were preselected before analysis and included disease stage at apheresis, age, sex, prelymphodepletion lactate dehydrogenase (LDH), prior systemic lines of therapy, disease histology (LCBL, FL, or MCL), absolute lymphocyte count at leukapheresis, Hispanic ethnicity, prelymphodepletion C-reactive protein (CRP), and prior autologous cellular transplant. Patient ID was included as a random effect, and variables were compared relative to their interaction with the time point. Time in days was defined as a discrete variable rather than a continuous variable to account for the time windows used during sample collection. A backward step regression was used for variable elimination before statistical analysis, and the least complex model was chosen. D7 values were used as the reference value. We also incorporated CAR AUC testing using the trapezoidal method to globally assess CAR19 exposure over the entire study period.

Survival package in R was used for determining univariate and multivariate survival methods using a Cox proportional hazards model.[23] Lasso regression was performed in glmnet using a Cox model,[24] and selective inference[25] was used to assign *P* values to variables selected by the lasso regression. Linear mixed effects modeling as described above was used to define CAR19 expansion by day.

Missing data

Missing CAR-FACS data were mainly attributed to the COVID-19 pandemic. Additional missing data points were considered as missing at random. Missing data were handled by linear mixed effects modeling by defining each patient as a slope of available data points. Linear mixed effects modeling reduces weighting based on the amount of data missing. A complete case design[26] that required at least 3 data points was implemented for AUC data because reduction in AUC values was associated with missing data points.

qPCR data analysis

qPCR was performed according to our previously published reports.[16]

Affymetrix mRNA analysis

Affymetrix messenger RNA (mRNA) data were downloaded from cBioPortal[27] and used without additional transformation. Cohorts were formed from samples labeled "DLBCL," "FL," and "MCL." The cBioPortal data set used was "mbn_mdacc_2013," the log normalized data file used was "data_mrna_affymetrix_microarray_zscores_ref_all_samples.txt," and the raw count data file used was "data_mrna_affymetrix_microarray.txt." Expression differences were assessed with an unadjusted Wilcoxon test using log normalized z scores.

This study was reviewed under the Stanford Institutional Review Board (IRB) for human subject research, and an IRB letter is available upon request.

Results

Patient characteristics

We prospectively followed 236 patients treated with CAR19 at Stanford (Table 1; data associated with the entire clinical correlative data set is contained in supplemental Files 1 and 2). The entire cohort consists of 191 patients treated for LBCL with axi-cel, 20 patients treated for FL with axi-cel, and 25 patients treated for MCL with brexu-cel. Of the 191 patients with LBCL, 11 (5.75%) were treated in second line. Ninety-eight percent of patients were treated as standard of care. Median follow-up time determined by reverse Kaplan-Meier was 23.85 months for the LBCL cohort, 14.65 months for the FL cohort, and 13.27 months for the MCL cohort. The 12-month PFS, TTP, and OS were 50.9%, 53.15%, and 75.27% for LBCL, 87.1%, 95%, and 87.1% for FL, and 66.9%, 69.8%, and 92% for MCL, respectively (Table 1; Figure 1A-B; supplemental Data Files 1-2). These results are comparable with the outcomes in the ZUMA-1, ZUMA-7, ZUMA-2, and ZUMA-5 studies.[1,3,8,9] Death from infection and second malignancy is an important topic and CAR19 research.[28,29] Of 116 PFS events in the entire cohort, 15 were due to nonrelapse mortality, including 12 attributable to infection and 3 attributable to second malignancy.

There was a significant difference in median age (63.0 years for LBCL, 60.5 for FL, and 68.0 for MCL) as well as median prior systemic lines of therapy (3.0 for LBCL, 4.5 for FL, and 4.0 for MCL) between the groups. The entire cohort was of 15.7% Hispanic ethnicity and 2.1% Black by self-identification. The LBCL cohort included 18.8% high-grade BCL (HGBCL) and 16.8% transformed FL (TFL). There were no differences in survival outcomes between patients with diffuse large B-cell lymphoma (DLBCL), HGBCL, and TFL, consistent with prior reports (supplemental Figure 1A).

Absolute CAR19 expansion is CD8 dominant and occurs over 7 orders of magnitude

To understand how CAR19 expansion across the subtypes of non-Hodgkin lymphoma (NHL) affects clinical outcomes, we prospectively collected patient blood on D7, D14, D21, and D28 (supplemental Figure 1B). In total, 639 samples were collected from 188 unique patients. There was a gap in data acquisition from March 2020 to March 2021 when routine sample processing was halted due to the COVID-19 pandemic (supplemental Figure 1C-D). There were no major differences between the population with and without CAR19 profiling, except an increase in the number of patients with MCL and FL after the later US Food and Drug Administration approval of CAR19 for these indications (supplemental Table 1). Utility of the flow cytometry assay was validated against 115 qPCR measurements of axi-cel across 35 individual patients, and values were highly correlated (Pearson coefficient, 0.52; $P < 0.0001$; supplemental Figure 1E-F).

CAR19 immune phenotyping allowed for the quantification of CD4+ and CD8+ CAR19 levels for longitudinal and AUC analysis. Median percent CAR at D7 was 14.67% of T cells (Figure 1C). This value dropped to a median of 1.33% by D28 indicating rapid loss of CAR19 as a percent of the T-cell population during the first 28 days. Absolute total CAR19 counts ranged over 7 orders of magnitude (Figure 1C) with median peak CAR19 expansion achieved on D14. The absolute CD4+ and CD8+ CAR19 counts were highly correlated (Spearman rho, 0.81; $P < 0.0001$; Figure 1D), suggesting comparable expansion of each population. There was a global CD8+ CAR19 predominance throughout the study period (Figure 1E), with a median CD4:CD8 ratio across time points of 0.62. The CD4+:CD8+ was reduced on D14 and D21 relative to day D7 but

Table 1. Study patient characteristics

Variable	LBCL	FL	MCL	*P* value
n	191	20	25	
Age at apheresis, median (IQR)	63 (55-71)	60.50 (53-69.25)	68 (65-73)	.025
Sex = female, n (%)	81 (42.4)	7 (35.0)	6 (24.0)	.188
ECOG, n (%)				.277
0	41 (21.5)	1 (5.0)	3 (12.0)	
1	133 (69.6)	17 (85.0)	21 (84.0)	
2+	17 (8.9)	2 (10.0)	1 (4.0)	
Identifies as Hispanic = Yes, n (%)	29 (15.2)	6 (30.0)	2 (8.0)	.119
Stage at apheresis, n (%)				.019
1	24 (12.6)	0 (0.0)	0 (0.0)	
2	24 (12.6)	1 (5.0)	1 (4.0)	
3	19 (9.9)	6 (30.0)	3 (12.0)	
4	124 (64.9)	13 (65.0)	21 (84.0)	
Prior auto transplant, n (%)	43 (22.5)	2 (10.0)	8 (32.0)	.213
Prior systemic lines, median (IQR)	3 (2-4)	4.50 (3-7.25)	4 (3, 6)	<.001
Normalized pre-LD LDH, median (IQR)	1.10 (0.84-1.49)	1.05 (0.88-1.32)	0.90 (0.82-1.26)	.334
ALC at leukapheresis, median (IQR)	0.78 (0.50-1.12)	0.76 (0.58-1.19)	1.17 (0.50-1.64)	.409
COO = non-GCB, n (%)	77 (42.1)	NA	NA	
Histology, n (%)				
DLBCL	110 (57.6)	NA	NA	
HGBCL	36 (18.8)	NA	NA	
TFL	32 (16.8)	NA	NA	
Other LBCL	13 (6.8)	NA	NA	
History of CNS disease, n (%)	14 (7.3)	0 (0.0)	3 (12.0)	.299

Patients are representative of prior reported cohorts and have similar outcomes to those reported in major studies and large consortia analysis. *P* values as assigned by unadjusted Kruskal-Wallis test.

ALC, absolute lymphocyte count; CNS, central nervous system; COO, cell of origin; ECOG, Eastern Cooperative Oncology Group; GCB, germinal center B-cell; IQR, interquartile range; LD, lymphodepletion; NA, not available.

was not significantly different on day D28 ($P < .05$ and $P < .01$, respectively, by Wilcoxon test; Figure 1E). These results suggest initial CD8+ CAR19 dominance and greater CD4+ cell persistence.

MCL histology is associated with increased CAR19 expansion

To understand how pretreatment variables affect CAR19 expansion longitudinally in humans, we used a multivariate linear mixed effects model to determine day-specific changes in CAR19 expansion (see "Methods"). Treatment with brexu-cel for MCL was associated with the highest CAR19 expansion compared with treatment with axi-cel for LBCL or FL. MCL demonstrated significant levels of CAR19 on D14, D21, and D28 ($P < .05$; $P < .01$; $P < .05$; Figure 2A). Median CAR19 counts for LBCL vs MCL on D14, D21, and D28 were as follows: 6.24 vs 21.7; 1.69 vs 6.87; and 1.01 vs 6.88 cells per μL. The AUC was significantly lower in LBCL than MCL ($P < .01$, Wilcoxon test; Figure 2B), with median LBCL AUC of 159.76 vs median MCL AUC of 649.39 (4.06-fold difference, days × cells per μL).

Differences in CAR19 were also identified within LBCL when compared with DLBCL, HGBCL, and TFL. There was no significant difference in day-specific CAR19 expansion levels by histology using multivariate mixed effects modeling with backward step regression (Figure 2C). There was a main effect difference between HGBCL and DLBCL before step elimination ($P = .05$). There was a significant difference in HGBCL vs DLBCL, with HGBCL histology having significantly lower CAR19 absolute expansion than DLBCL histology ($P < .05$, Wilcoxon test; Figure 2D).

Our analysis also demonstrated that higher prelymphodepletion LDH correlated with increased CAR19 persistence on D7, D14, and D21 ($P < .05$; $P < .01$; and $P < .05$, respectively). Exploratory analysis of these differences indicated that increased persistence was largely driven by the highest quartile of LDH (Figure 2E). However, there was no AUC difference in patients above or below the upper limit of normal (Figure 2F). Patients with older age had reduced CAR19 persistence on D21 and D28 in the mixed effects model that was similarly driven by the highest quartile age bracket ($P < .001$; Figure 2G). Similarly, there was no AUC difference between older and younger patients using standard thresholds (Figure 2H).

The effect size of the differences noted in the LDH and age variables were substantially smaller than that of the histology difference for the MCL histology. These variables also did not have an

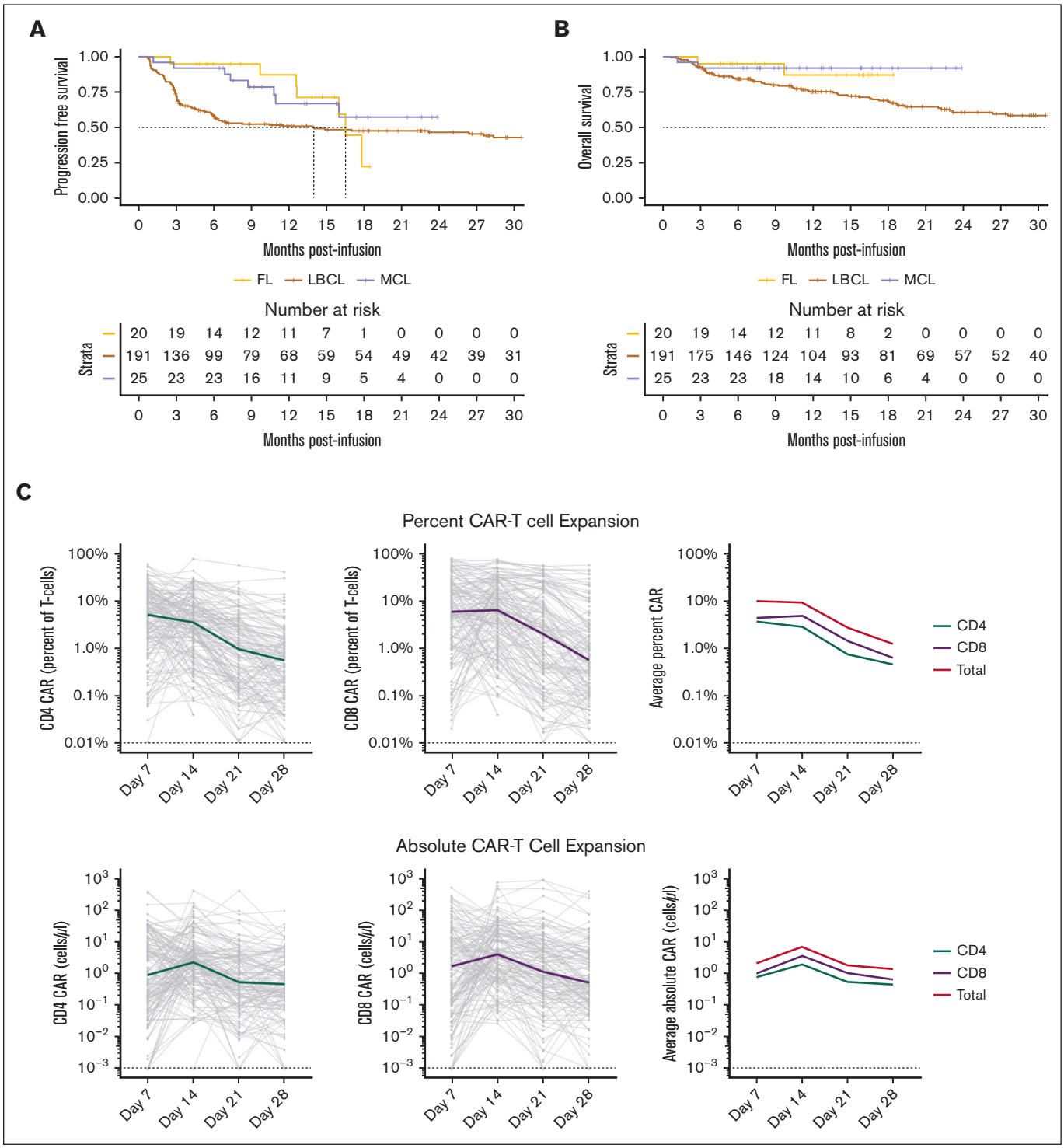

Figure 1. CAR-FACS analysis measures CAR19 expansion across histologic subtypes over 7 orders of magnitude. (A-B) PFS and OS curves in Stanford's CAR19 cohort for LBCL, FL, and MCL are representative of published results. Dotted lines represent respective median time to event. Only the first 30 months of follow-up are illustrated. (C) Percent and absolute plots of longitudinal CAR19 expansion in the first month demonstrates CAR19s expand over 7 orders of magnitude with CD8 dominance. Dotted lines represent theoretical limits of detection based on prior assay calibration. (D) Absolute CD4 and CD8 CAR19 counts are highly correlated during expansion. (E) There is a small relative increase in CD8 CAR19 expansion at D14 and D21 with increasing persistence of the CD4 CAR19 at D28 (Wilcoxon test). $^*P < .05$, $^{**}P < .01$.

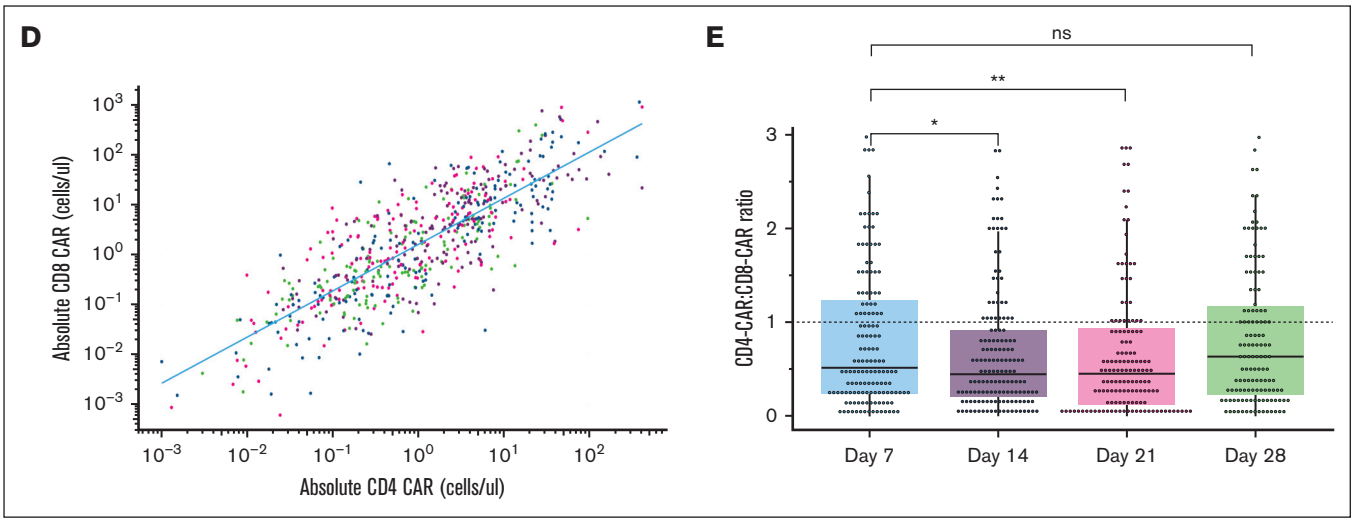

Figure 1 (continued)

AUC difference in evaluable patients, indicating no major differences in total CAR19 exposure. We therefore interpret MCL histology as the major pretreatment driver of CAR19 expansion in this data set. In total, our CAR-FACS data show CAR19 expansion is disease histology dependent; specifically, there is increased CAR19 expansion and persistence in patients treated with brexucel for MCL.

To better understand why MCL has greater CAR19 expansion, we analyzed a microarray data set[30,31] publicly available on cBioPortal[27] that includes 95 DLBCL, 65 FL, and 43 MCL specimens (see "Methods"). In this data set, log-transformed and z score–normalized *CD19* expression in MCL is significantly increased relative to DLBCL (supplemental Figure 2A). Median raw Affymetrix counts in the same data set for MCL was 654.59, for DLBCL was 294.66, and for FL was 377.02. Although inconclusive by itself, these data suggest that MCL may have greater surface antigen density of CD19 to drive expansion.

Patients treated for MCL experience greater toxicity

Because CAR19 expansion was previously associated with toxicity, we hypothesized our patients with MCL would experience greater toxicity than patients with LBCL. Stanford follows standard toxicity algorithms based on cohort 4 of the ZUMA-1 study[32] that are the same for all patients treated with axi-cel and brexu-cel. The most current treatment algorithm began in March 2020, and the first patient with MCL was treated in October 2020. As such, we compared patients with LCBL, MCL, and FL treated from March 2020 until the end of the study to determine the differences in toxicity.

Consistent with increased CAR19 exposure, patients with MCL had significantly increased frequencies of high-grade ICANS compared with patients with LBCL (36% grade 3-4 ICANS vs 14.2%; $P < .05$, Kruskal-Wallis test; Table 2). The median cumulative dose of steroid exposure after infusion (in mg of dexamethasone) for patients with MCL was 4.02-fold higher than that for those with LBCL (85 mg in LBCL vs 342 mg in MCL; $P < .05$, Kruskal-Wallis test), and 88% of patients with MCL required tocilizumab compared with 77.4% of patients with LBCL. The median hospital stay was 15 days for patients with MCL, whereas it was 13 days for patients with LCBL and 12 days for patients with FL ($P < .05$, Kruskal-Wallis test). There was no difference in the rates of CRS. In sum, patients with MCL in our cohort experienced high severity of ICANS, more steroid and tocilizumab exposure, and longer hospital stays than patients with LBCL and FL.

CAR19 expansion is associated with all major CAR19 toxicities in the first month of treatment

We compared CAR19 AUC with CAR19-related toxicities, including CRS grade, ICANS grade, and the need for G-CSF after D14. G-CSF is given for patients with ANC <1000, making this end point a surrogate measurement of prolonged neutropenia. We found that CAR19 AUC was significantly associated with increased severity of CRS grade, ICANS grade, and the need for G-CSF after D14 ($P < .0001$; $P < .001$; and $P < .01$, respectively, by Wilcoxon test; Figure 3A-D).

We also measured the CD4+:CD8+ ratio as AUC values to determine how this ratio associates CAR19-related toxicities. The CD4+:CD8+ ratio was significantly lower in patients with severe (grade 3-4) ICANS than those with either less severe (grade 1-2) ICANS or without ICANS ($P < .001$ comparing CD4+:CD8+ CAR19 ratio in patients without ICANS and patients with grade 3-4 ICANS, Wilcoxon test; Figure 3B). There were no differences in CD4+:CD8+ ratio associated with CRS or G-CSF after D14.

Patients with MCL have the greatest CAR19 expansion with corresponding increases in toxicity (Figure 2A). To understand the relative contribution of CAR19 expansion vs histology, we performed a multivariate ordinal regression analysis (see "Methods"). Additionally, we included D7 CAR19 expansion (log10 cells per μL) as well as D7 CD4+:CD8+ CAR19 ratio. Only D7 CAR expansion and patient age were associated with increased ICANS after variable elimination by step backward regression ($P < .001$ for CAR19 expansion; $P < .05$ for age; supplemental Figure 2B). Moreover, even when all patients who developed ICANS before D7 were removed from this model and the same analysis was

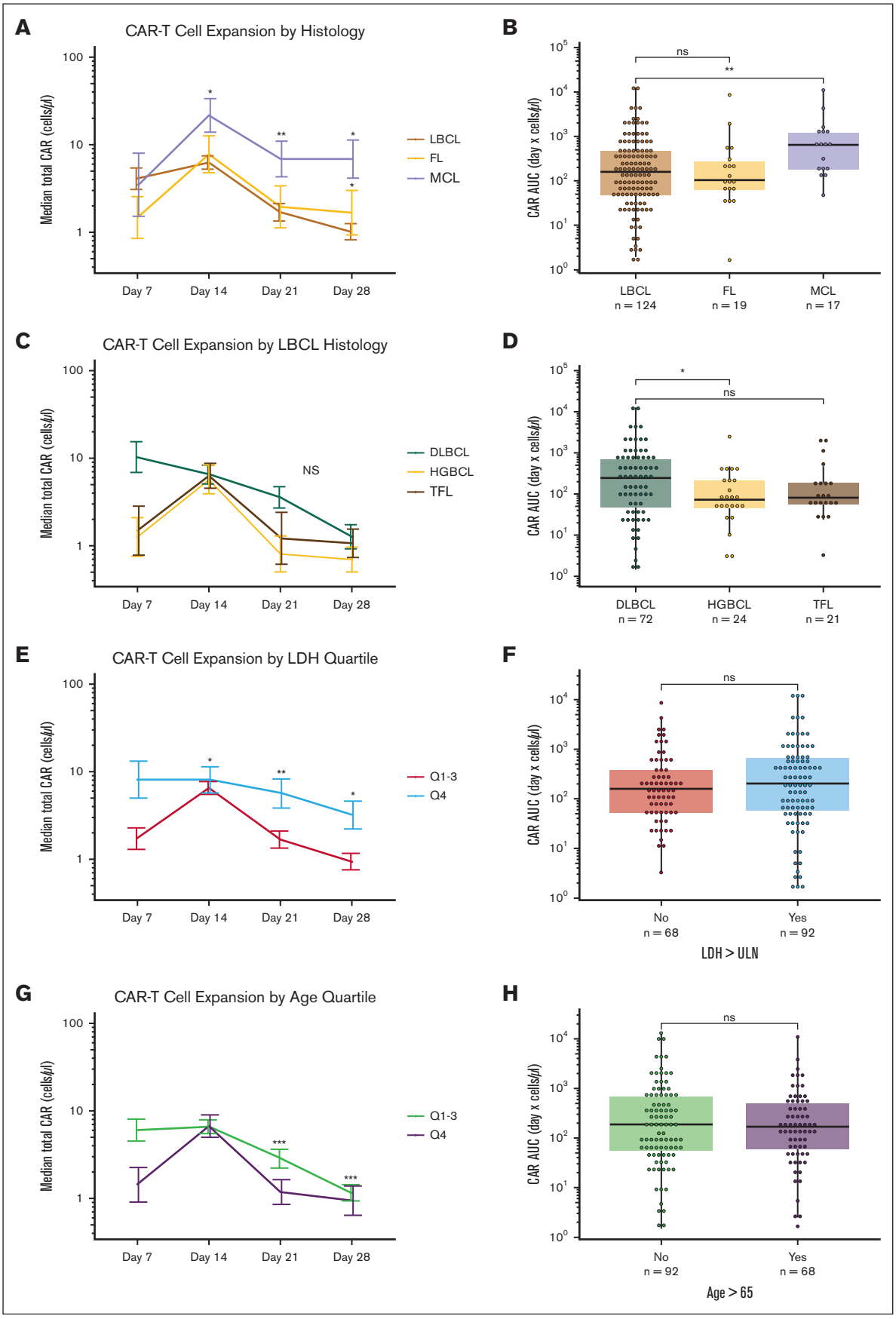
A
CAR-T Cell Expansion by Histology
Median total CAR (cells/μl)
100
10
1
Day 7
Day 14
Day 21
Day 28
LBCL
FL
MCL
B
CAR AUC (day x cells/μl)
ns
**
LBCL
n = 124
FL
n = 19
MCL
n = 17
C
CAR-T Cell Expansion by LBCL Histology
NS
DLBCL
HGBCL
TFL
D
*
ns
DLBCL
n = 72
HGBCL
n = 24
TFL
n = 21
E
CAR-T Cell Expansion by LDH Quartile
Q1-3
Q4
F
No
n = 68
Yes
n = 92
LDH > ULN
G
CAR-T Cell Expansion by Age Quartile
***
H
No
n = 92
Yes
n = 68
Age > 65

Figure 2.

Table 2. Toxicity outcomes by disease histology

Histology	LBCL	FL	MCL	*P* value
n	106	20	25	
CRS grade 2-3, n (%)	57 (53.8)	7 (35.0)	17 (68.0)	.088
Day maximum CRS, median (IQR)	4 (2-6)	5.00 (4-7)	4 (2-6.25)	.19
Length of CRS, median (IQR)	4 (3-6)	4 (3-6)	3 (2-4.25)	.135
Max ICANS grade, n (%)				.043
0	54 (50.9)	11 (55.0)	8 (32.0)	
1-2	37 (34.9)	3 (15.0)	8 (32.0)	
3-4	15 (14.2)	6 (30.0)	9 (36.0)	
Day maximum ICANS, median (IQR)	6 (5-8)	8 (7-10)	3 (2-3)	<.001
Length ICANS, median (IQR)	3 (1-6)	3 (1-5)	5 (1-11)	.254
G-CSF after D14, n (%)	54 (50.9)	10 (50.0)	14 (56.0)	.89
Cumulative steroid dose, median (IQR)	85 (10-199)	15 (0-343.5)	342 (91-442)	.014
Tocilizumab doses, median (IQR)	1 (1-2)	1 (0-2)	1 (1-2)	.14
Required tocilizumab, n (%)	82 (77.4)	11 (55)	22 (88.0)	.031
Length of hospital stay, median (IQR)	13 (11-15.75)	12 (9-15)	15 (13-22)	.01

Patients treated for MCL have significantly greater rates of severe ICANS and more frequent treatment with tocilizumab, require substantially more steroids, and have longer hospital stays than patients treated for FL and LBCL. *P* values as assigned by unadjusted Kruskal-Wallis test.
IQR, interquartile range; Max, maximum.

performed, increased CAR19 expansion was again significantly associated with the development of ICANS ($P < .01$). From these analyses, we conclude that CAR19 expansion is the variable most strongly associated with ICANS.

CAR19 expansion measured by peripheral blood immune phenotyping is not associated with improved survival outcomes

We used a univariate Cox proportional hazards model to define association between CAR19 expansion and the pre-established end point of PFS in the LBCL cohort. There was no association between CAR19 AUC and PFS. Among the 27 selected variables, the only significant variables associated with worse survival outcomes in univariate analysis were higher preinfusion LDH ($P < 0.0001$), need for bridging therapy ($P < .05$), higher prelymphodepletion CRP ($P < .001$), and refractory disease at referral ($P < .05$). No covariates were associated with improved PFS outcomes (a list of all variables included in Cox analysis is available in supplemental File 3). Using univariate D7 CAR expansion in isolation (n = 134) also did not have significant association with PFS ($P = .32$, univariate Cox proportional hazards model).

Additionally, neither CAR19 AUC nor CAR19 peak expansion was associated with best response measured as complete response vs partial response, stable disease, or progressive disease (supplemental Figure 3A-B). Similarly, there was no difference in CAR19 AUC or CAR19 peak expansion in patients with and without progression (supplemental Figure 3C-D).

We hypothesized that CAR19 expansion may interact with pretreatment risk to define higher or lower risk groups. LDH measured before lymphodepletion is the most consistent variable associated with outcomes across multiple publications.[15,16,33-35] Prelymphodepletion LDH is also strongly associated with preinfusion circulating tumor DNA (ctDNA) in a subset of patients in our cohort (Spearman rank correlation coefficient = 0.65 between LDH and preinfusion ctDNA; $P < 0.0001$; Figure 4A).[15] As such, we tested the interaction between CAR19 expansion and prelymphodepletion LDH using a lasso regression relative to the variables used in the univariate Cox analysis. We bisected the data set using median prelymphodepletion LDH (median, 1.1 × upper limit of normal) and median CAR19 AUC to generate 4 interaction terms (CAR^{low}/LDH^{low}, CAR^{low}/LDH^{high}, CAR^{high}/LDH^{low}, and

Figure 2. CAR19 expansion is dependent on lymphoma histology. (A) MCL histology has increased D14, D21, and D28 CAR19 expansion relative to LBCL based on a multivariate linear mixed effects model of longitudinal data. (B) CAR19 AUC in MCL is greater than LBCL with almost fourfold higher CAR19 exposure (Wilcoxon test). (C-D) Breakdown of the LBCL histology indicates there are differences between HGBCL, TFL, and other LBCL pathologies in CAR19 expansion. These differences are not significant in mixed effects modeling (C) but there is a significant AUC difference between HGBCL and other lymphoma histologic subtypes when directly compared (D; Wilcoxon test). (E) Greater LDH is associated with significantly more persistence of CAR19s on D21 and D28 using a multivariate mixed effects model. Plot is representative of statistical output that uses continuous values. (F) Discrete analysis of CAR19 expansion (Wilcoxon test) by AUC based off prelymphodepletion LDH greater than the upper limit of normal does not demonstrate statistically significant total exposure differences in CAR19 expansion. (G) Greater age is associated with reduced CAR19 persistence on D21 and D28 using the same modeling. Plot is representative of statistical results that uses continuous values. (H) Discrete modeling of total CAR19 exposure over the first 28 days does not demonstrate significant differences in AUC using a standard age threshold (Wilcoxon test). However, highly significant effect sizes in mixed effects modeling for both LDH and age were modest. $^*P < .05$; $^{**}P < .01$, $^{***}P < 0.001$; ns; error bars are standard error of the mean; plots are representative of modeling results. Significance values in line charts represent the interaction between CAR19 expansion and day; graphs are only representative of the continuous statistics. ns, not significant.

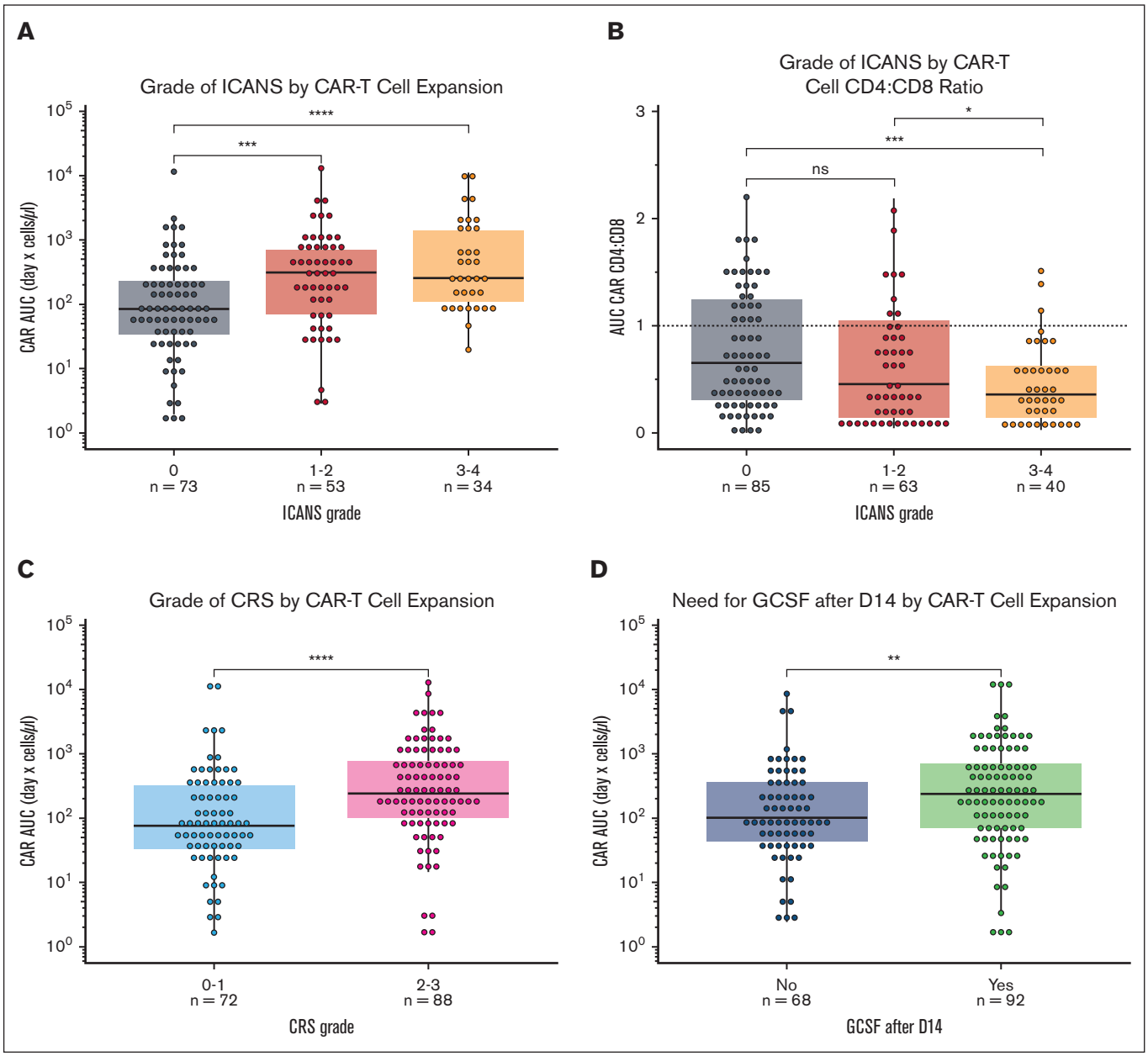

Figure 3. CAR19 expansion is associated with CAR19-mediated toxicity. (A) CAR19 expansion defined by AUC is significantly associated with the development of severe ICANS. (B) Lower CAR19 CD4:CD8 ratio is also associated with the development of severe ICANS. (C) Increased CAR19 expansion is associated with more severe CRS. (D) Increased CAR19 expansion is associated with the need for G-CSF after D14. *$P < .05$; **$P < .01$; ***$P < .001$; ****$P < .0001$. All significance values represent Wilcoxon testing.

CAR^{high}/LDH^{high}). We then used selective inference[36] to generate P values associated with each selected lasso variable (Figure 4B).

Prelymphodepletion LDH and CRP were selected in the lasso as contributing to inferior PFS outcomes ($P = .068$ and $P = .01$, respectively; alpha significance for this analysis <0.1). The CAR^{low}/LDH^{high} population and need for bridging therapy were selected by the lasso as having inferior PFS outcomes but was not significant ($P = .86$ and $P = .63$). The former finding may suggest that in patients with high tumor burden, increased CAR expansion is necessary to establish disease control. Interestingly, the interaction between CAR19 expansion below median and LDH below median (CAR^{low}/LDH^{low}) was also selected as contributing to superior PFS outcomes (hazard ratio, 0.36; $P < .05$; Figure 4C). Results of risk stratification by CAR/LDH are represented as a Kaplan-Meier plot in Figure 4C.

This result was unexpected because it indicated patients in the low LDH risk group who also had low CAR19 expansion did significantly better than other patient groups. To understand this difference, we compared patients in the CAR^{low}/LDH^{low} group with patients in the CAR^{high}/LDH^{low} group (Table 3; supplemental Table 2; supplemental Figure 3E). The groups were similar in composition, although there was a trend for lower stage at

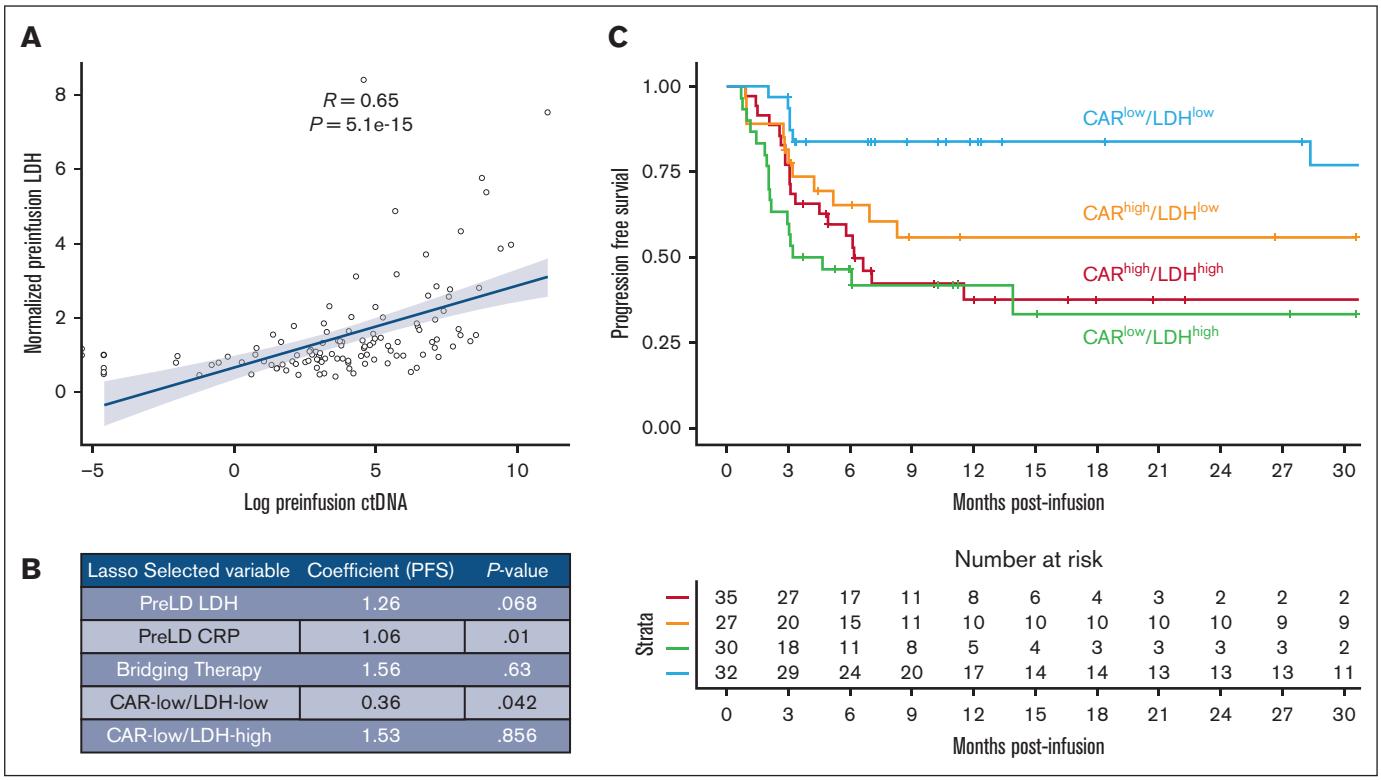

Lasso Selected variable	Coefficient (PFS)	*P*-value
PreLD LDH	1.26	.068
PreLD CRP	1.06	.01
Bridging Therapy	1.56	.63
CAR-low/LDH-low	0.36	.042
CAR-low/LDH-high	1.53	.856

Figure 4. The interaction between pretreatment risk by LDH and CAR19 expansion classifies patients with high and low risks. (A) Pretreatment LDH strongly correlates with pretreatment ctDNA. (B) Results of lasso regression incorporating the interaction between prelymphodepletion LDH (greater or less than data set median) and prelymphodepletion CAR AUC (greater or less than data set median). Expected values selected by the lasso based on prior publications include prelymphodepletion LDH, pre-LD CRP, and bridging therapy. In addition, patients with high LDH and low CAR19 expansion (CAR^{low}/LDH^{high}) are selected as doing worse, whereas patients with low LDH and low CAR19 expansion (CAR^{low}/LDH^{low}) are selected as having improved outcomes. (C) Kaplan-Meier estimate of patients stratified by LDH and CAR expansion demonstrate superior outcomes by PFS in patients with low LDH and low CAR19 expansion.

apheresis in the CAR^{low}/LDH^{low} group (supplemental Table 2). There was no difference in prelymphodepletion LDH or preinfusion ctDNA in evaluable patients (supplemental Table 2). We found that patients in the CAR^{high}/LDH^{low} group had significantly higher rates of severe CRS and ICANS with associated increases in cumulative steroid dose than the CAR^{low}/LDH^{low} group (Table 3). There was nominally greater nonrelapse mortality (4 vs 0 nonrelapse deaths) in this group as well, although this value was not significant (Fisher test). When directly compared, PFS was worse in the CAR^{high}/LDH^{low} group than the CAR^{low}/LDH^{low} group by Cox modeling (supplemental Figure 3E).

Overall, our data suggest that blood CAR19 expansion is associated with toxicity but not predictive of PFS. Instead, in patients who risk stratify into lower risk groups by LDH, lower CAR19 expansion was associated with improved outcomes, possibly due in part to lower toxicity.

Discussion

This single institution study prospectively assessed patients across multiple lymphoma histologic subtypes treated with axi-cel and brexu-cel by immune phenotyping to directly assess the relevance of CAR19 surface receptor expression on clinical outcomes.

We found histology is a primary driver of CAR19 expansion in standard of care patients. Although we observed that CAR19 expansion is increased in patients with MCL, the cause of this is unclear. This observation could be due to product differences (brexu-cel vs axi-cel), the histology itself, or possibly prior treatments such as the use of ibrutinib, which can protect T cells from

Table 3. Comparison of patients with high CAR exposure and low LDH vs patients with low CAR exposure and low LDH

Variable	CAR^{low}/LDH^{low}	CAR^{high}/LDH^{low}	*P* value
n	32	27	
Max ICANS, n (%)			.001
0	22 (68.8)	7 (25.9)	
1-2	5 (15.6)	16 (59.3)	
3-4	5 (15.6)	4 (14.8)	
Tocilizumab = yes, n (%)	19 (59.4)	25 (92.6)	.009
Cumulative steroid dose, median (IQR)	20 (0-121)	150 (35-210)	.016
CRS grade 2-3, n (%)	14 (43.8)	20 (74.1)	.037

Patients with low CAR19 exposure in the lower risk group have improved safety characteristics including less CRS and ICANS and lower total steroid use. *P* values as assigned by unadjusted Kruskal-Wallis test.
IQR, interquartile range; Max, maximum.

senescence in specific contexts.[37] Using a separate mRNA microarray data set, we do find that MCL CD19 expression is significantly higher than that of DLBCL and FL. CD19 mRNA and protein expression is previously shown to correlate, indicating increased antigen availability is a possible mechanism for the observed increase in expansion.[38] Interestingly, CAR19 expansion was lower in HGBCL histology than DLBCL, and the cause of this too is unclear. Interaction between CAR and tumor histology may be driven by location and extent of disease or antigen density on the tumor itself. Further study is warranted.

Many groups have shown LDH is a surrogate for disease burden,[15,16,33-35,39] and here, we find that elevated LDH associates with increased CAR19 persistence. We hypothesize that greater tumor burden results in more exposure to CD19 antigen, which likely drives CAR19 persistence. Moreover, we find that increasing age leads to reduced CAR19 persistence. The impact of this finding is unclear. Older patients have improved PFS in a multivariate model[35]; however, based on our results, this finding does not appear to be due to CAR19 persistence.

Cross trial comparisons of patients with MCL vs DLBCL suggested higher rates of ICANS in patients with MCL. Our study across histologic types directly shows the higher rate of severe ICANS in patients with MCL. Moreover, we found that patients with MCL required 4 times the cumulative steroid dose and had longer hospitalization than patients treated for LBCL or FL. We postulate that the increased CAR19 expansion in MCL directly informs why these patients have increased relative toxicity, which has been a major ongoing question in CAR19 research.

By a multivariate model, we found that CAR19 expansion was most strongly associated with the development of ICANS among the variables tested including histology. This analysis demonstrated that expansion kinetics is the major factor associated with toxicity, and it is likely that the increased toxicity noted in patients with MCL is due directly to increased CAR19. Reduced CD4+:CD8+ ratio was also significantly associated with ICANS, which, to our knowledge, is the first such report of CAR CD4+:CD8+ ratio associated with outcomes. Monitoring blood expansion of CAR19 may allow for the identification of patient at high risk of ICANS.

Our analysis of CAR19 expansion did not associate with durable response. This is in contrast to prior reports using qPCR and cfDNA that have found an association between CAR19 expansion on outcomes.[1,4,6,15,40] Another study restricted to patients with LBCL treated with tisagenlecleucel ([tisa-cel] n = 40) and axi-cel (n = 23) found flow cytometric evidence of associating increased CAR19 expansion with improved outcomes, although vectors differences could account for this discrepancy.[41-43] Other studies have failed to demonstrate an association between CAR19 expansion and improved efficacy.[3,44] Overall, CAR19 expansion did not associate with efficacy in our study. Interestingly, however, low CAR19 expansion was associated with better PFS in patients with low tumor burden (ie, low LDH). There was also association of patients with high tumor (ie, high LDH) having improved outcomes with more expansion selected in the lasso regression, although this association was not significant after selective inference analysis. These data suggest that CAR19 expansion needs to match tumor burden, and excess CAR19 expansion is dispensable to outcomes possibly due in part to increased toxicity.

The clinical differences noted in this study in comparison with other studies may be due to the method of measuring CAR19 cell surface receptor directly in the blood by anti-idiotype. Other methods to monitor CAR19, such as cfDNA analysis, may allow for the detection of CAR19 expansion within tissue or tumor.[15] Our study also includes patients treated in earlier lines of therapy, so total disease burden may be less than in original reports, which may change the nature of tumor-CAR interaction. Of note, CAR19 blood expansion did not associate with efficacy in frontline ZUMA-12 study[44] and did not associate with duration and depth of response in the ZUMA-7 study.[45]

In conclusion, our single institution flow cytometry immunophenotypic quantification of CAR19 expansion in 188 patients across multiple histologic types shows CAR19 expansion associates with CRS and ICANS toxicity but not efficacy. Lymphoma histology drives this expansion, leading to histology-specific variation in toxicity.

Acknowledgments

D.B.M. is funded by Program Project Grant P01 CA049605 and Kite sponsored research. M.P.H. is a fellow of the Leukemia and Lymphoma Society. A.A.A. is a scholar of the Leukemia and Lymphoma Society and is the Moghadam Family Professor of Medicine at Stanford University.

Authorship

Contribution: M.P.H. was involved in study design, study analysis, clinical data collection, and article and figure generation; E.C. was involved in study design and analysis; C.G. and A.M. were involved in study design, study analysis, and clinical data collection; N.K. was involved in study design, study analysis, clinical data collection, and manuscript editing; Z.E. and S. Syal were involved in flow cytometry data generation and analysis; Z.G., B. Sworder, J.S.-M., J.T., and Y.L. were involved in study design and study analysis; L.M., R.S.N., and S.A. were involved in clinical data collection; R.L. was involved in study design, study analysis, and clinical data collection; E.M., A.R.R., J.S., W.-K.W., P.S., S. Sidana, and S.B. were involved in clinical data collection; M.S. was involved in clinical data collection and manuscript editing; S.D. was involved in clinical data collection; B. Sahaf was involved in study design, study analysis, flow cytometry data generation, and analysis; D.M.K., C.L.M., and R.T. were involved in study design and study analysis; M.J.F. was involved in study design, study analysis, and clinical data collection; A.A.A. was involved in study design and study analysis; and D.B.M. was involved in study conception, funding, design, and analysis, and clinical data collection.

Conflict-of-interest disclosure: M.P.H. served on an advisory board for Kite Pharmaceuticals. Z.G. is an inventor on 2 patent applications; holds equity in Boom Capital Ventures; and is a consultant for Mubadala Ventures. S.B. reports consulting for Allogene. C.L.M. is a founder, equity holder, consultant, and director of Cargo Therapeutics and Link Cell Therapies; reports equity in Lyell Immunopharma and royalties from the National Institutes of Health for CAR22; and consults for Immatics, Ensoma, Mammoth, Adaptimmune, and Bristol Myers Squibb. L.M. reports research support from Adaptive Biotechnologies and Servier Laboratories, and consults for Amgen and Pfizer. P.S. reports research support from Kite Pharma-Gilead. S. Sidana reports consulting for Janssen. D.M.K. reports consultancy for Roche, Adaptive Biotechnologies, and Genentech, and equity

ownership interest in Foresight Diagnostics. A.A.A. reports consulting for and having stock options in CiberMed; consulting fees and research funding from Celgene; holding stock options in CAPP Medical; consulting fees, honoraria, and travel funding from Roche; holding stop options in Forty Seven; holding stock options in Syncopation Life Sciences; consulting fees and travel fund from Gilead; consulting fees from and holding stock options in Foresight Diagnostics; honoraria from Jannsen; and consulting for Lymphoma research foundation. M.J.F. reports consulting for Kite Pharma-Gilead, Adaptative Biotechnologies, and Cargo Therapeutics, and research support from Kite Pharma-Gilead, Allogene Therapeutics, Cargo Therapeutics, and Adaptative Biotechnologies. D.B.M. reports consulting for Kite Pharma-Gilead, Juno Therapeutics-Celgene, Novartis, Janssen, and Pharmacyclics, and research support from Kite Pharma-Gilead, Allogene Therapeutics, Cargo Therapeutics, Pharmacyclics, Miltenyi Biotec, and Adaptive Biotechnologies. The remaining authors declare no competing financial interests.

ORCID profiles: C.G.S., 0000-0001-7643-8154; N.K., 0000-0003-0723-7919; S. Syal, 0009-0008-6992-8815; Z.G., 0000-0003-2343-5771; Y.L., 0000-0002-7698-8962; L.M., 0000-0002-9887-6136; S.A., 0000-0003-1993-4172; P.S., 0000-0002-6721-0358; S. Sidana, 0000-0003-3288-7614; M.S., 0000-0002-2702-0381; D.M.K., 0000-0002-6382-4651; C.L.M., 0000-0003-0359-9023; A.A.A., 0000-0002-5153-5625; D.B.M., 0000-0003-0717-4305.

Correspondence: Matthew J. Frank, Division of Blood and Marrow Transplantation and Cellular Therapy, Department of Medicine, Stanford University School of Medicine, 300 Pasteur Dr, Room H0145, Stanford, CA 94305; email: mjfrank@stanford.edu; David B. Miklos, Division of Blood and Marrow Transplantation and Cellular Therapy, Department of Medicine, Stanford University School of Medicine, 269 West Campus Dr, CCSR 2205, Stanford, CA 94305; email: dmiklos@stanford.edu; and Ash A. Alizadeh, Divisions of Oncology and Hematology, Department of Medicine, Cancer Institute, Institute for Stem Cell Biology and Regenerative Medicine, Stanford University School of Medicine, Lorry Lokey Building, SIM1, Room G2120B, 265 Campus Dr, Stanford, CA 94305; email: arasha@stanford.edu.

References

1. Neelapu SS, Locke FL, Bartlett NL, et al. Axicabtagene ciloleucel CAR T-cell therapy in refractory large B-cell lymphoma. *N Engl J Med*. 2017;377(26):2531-2544.
2. Locke FL, Ghobadi A, Jacobson CA, et al. Long-term safety and activity of axicabtagene ciloleucel in refractory large B-cell lymphoma (ZUMA-1): a single-arm, multicentre, phase 1–2 trial. *Lancet Oncol*. 2019;20(1):31-42.
3. Locke FL, Miklos DB, Jacobson CA, et al; All ZUMA-7 Investigators and Contributing Kite Members. Axicabtagene ciloleucel as second-line therapy for large B-cell lymphoma. *N Engl J Med*. 2022;386(7):640-654.
4. Abramson JS, Palomba ML, Gordon LI, et al. Lisocabtagene maraleucel for patients with relapsed or refractory large B-cell lymphomas (TRANSCEND NHL 001): a multicentre seamless design study. *Lancet*. 2020;396(10254):839-852.
5. Schuster SJ, Bishop MR, Tam CS, et al. Tisagenlecleucel in adult relapsed or refractory diffuse large B-cell lymphoma. *N Engl J Med*. 2019;380(1):45-56.
6. Kamdar M, Solomon SR, Arnason J, et al. Lisocabtagene maraleucel versus standard of care with salvage chemotherapy followed by autologous stem cell transplantation as second-line treatment in patients with relapsed or refractory large B-cell lymphoma (TRANSFORM): results from an interim analysis of an open-label, randomised, phase 3 trial. *Lancet*. 2022;399(10343):2294-2308.
7. Westin JR, Oluwole OO, Kersten MJ, et al. Survival with axicabtagene ciloleucel in large B-cell lymphoma. *N Engl J Med*. 2023;389(2):148-157.
8. Wang M, Munoz J, Goy A, et al. KTE-X19 CAR T-cell therapy in relapsed or refractory mantle-cell lymphoma. *N Engl J Med*. 2020;382(14):1331-1342.
9. Jacobson CA, Chavez JC, Sehgal AR, et al. Axicabtagene ciloleucel in relapsed or refractory indolent non-Hodgkin lymphoma (ZUMA-5): a single-arm, multicentre, phase 2 trial. *Lancet Oncol*. 2022;23(1):91-103.
10. Fowler NH, Dickinson M, Dreyling M, et al. Tisagenlecleucel in adult relapsed or refractory follicular lymphoma: the phase 2 ELARA trial. *Nat Med*. 2022;28(2):325-332.
11. Hines MR, Knight TE, McNerney KO, et al. Immune effector cell-associated hemophagocytic lymphohistiocytosis-like syndrome. *Transplant Cell Ther*. 2023;29(7):438.e1-438.e16.
12. Neelapu SS, Tummala S, Kebriaei P, et al. Chimeric antigen receptor T-cell therapy – assessment and management of toxicities. *Nat Rev Clin Oncol*. 2018;15(1):47-62.
13. Baird JH, Epstein DJ, Tamaresis JS, et al. Immune reconstitution and infectious complications following axicabtagene ciloleucel therapy for large B-cell lymphoma. *Blood Adv*. 2021;5(1):143-155.
14. Wudhikarn K, Perales M-A. Infectious complications, immune reconstitution, and infection prophylaxis after CD19 chimeric antigen receptor T-cell therapy. *Bone Marrow Transplant*. 2022;57(10):1477-1488.
15. Sworder BJ, Kurtz DM, Alig SK, et al. Determinants of resistance to engineered T cell therapies targeting CD19 in large B cell lymphomas. *Cancer Cell*. 2022;41(1):210-225.e5.
16. Good Z, Spiegel JY, Sahaf B, et al. Post-infusion CAR TReg cells identify patients resistant to CD19-CAR therapy. *Nat Med*. 2022;28(9):1860-1871.
17. Cheson BD, Fisher RI, Barrington SF, et al. Recommendations for initial evaluation, staging, and response assessment of Hodgkin and non-Hodgkin lymphoma: the Lugano classification. *J Clin Oncol*. 2014;32(27):3059-3068.

18. Lee DW, Santomasso BD, Locke FL, et al. ASTCT Consensus grading for cytokine release syndrome and neurologic toxicity associated with immune effector cells. *Biol Blood Marrow Transplant*. 2019;25(4):625-638.

19. Spiegel JY, Patel S, Muffly L, et al. CAR T cells with dual targeting of CD19 and CD22 in adult patients with recurrent or refractory B cell malignancies: a phase 1 trial. *Nat Med*. 2021;27(8):1419-1431.

20. Jena B, Maiti S, Huls H, et al. Chimeric antigen receptor (CAR)-specific monoclonal antibody to detect CD19-specific T cells in clinical trials. *PLoS One*. 2013;8(3):e57838.

21. Bates D, Mächler M, Bolker B, Walker S. Fitting linear mixed-effects models using lme4. *J Stat Softw*. 2015;67(1):1-48.

22. Kuznetsova A, Brockhoff PB, Christensen RHB. lmerTest package: tests in linear mixed effects models. *J Stat Softw*. 2017;82(13):1-26.

23. Therneau T. A package for survival analysis in R. R Package version 3.5-8. 2024. Accessed 5 April 2024. https://CRAN.R-project.org/package=survival

24. Friedman JH, Hastie T, Tibshirani R. Regularization paths for generalized linear models via coordinate descent. *J Stat Softw*. 2010;33(1):1-22.

25. Tibshirani RJ, Taylor J, Lockhart R, Tibshirani R. Exact post-selection inference for sequential regression procedures. *Journal of the American Statistical Association*. 2016;111(514):600-620.

26. Hughes RA, Heron J, Sterne JAC, Tilling K. Accounting for missing data in statistical analyses: multiple imputation is not always the answer. *Int J Epidemiol*. 2019;48(4):1294-1304.

27. Cerami E, Gao J, Dogrusoz U, et al. The cBio cancer genomics portal: an open platform for exploring multidimensional cancer genomics data. *Cancer Discov*. 2012;2(5):401-404.

28. Spiegel JY, Jain MD, Nastoupil LJ, et al. Five year outcomes of patients with large B-cell lymphoma treated with standard-of-care axicabtagene ciloleucel: results from the US Lymphoma CAR-T Cell Consortium. *Blood*. 2023;142:1032.

29. Verdun N, Marks P. Secondary cancers after chimeric antigen receptor T-cell therapy. *N Engl J Med*. 2024;390(7):584-586.

30. Man Chun John M, Saber T, Alyssa B, et al. Pathognomonic and epistatic genetic alterations in B-cell non-Hodgkin lymphoma. *bioRxiv*. Preprint posted online 19 June 2019. https://doi.org/10.1101/674259

31. Ma MCJ, Tadros S, Bouska A, et al. Subtype-specific and co-occurring genetic alterations in B-cell non-Hodgkin lymphoma. *Haematologica*. 2021;107(3):690-701.

32. Topp MS, van Meerten T, Houot R, et al. Earlier corticosteroid use for adverse event management in patients receiving axicabtagene ciloleucel for large B-cell lymphoma. *Br J Haematol*. 2021;195(3):388-398.

33. Vercellino L, Di Blasi R, Kanoun S, et al. Predictive factors of early progression after CAR T-cell therapy in relapsed/refractory diffuse large B-cell lymphoma. *Blood Adv*. 2020;4(22):5607-5615.

34. Rabinovich E, Pradhan K, Sica RA, et al. Elevated LDH greater than 400 U/L portends poorer overall survival in diffuse large B-cell lymphoma patients treated with CD19 CAR-T cell therapy in a real world multi-ethnic cohort. *Exp Hematol Oncol*. 2021;10(1):55.

35. Nastoupil LJ, Jain MD, Feng L, et al. Standard-of-care axicabtagene ciloleucel for relapsed or refractory large B-cell lymphoma: results from the US Lymphoma CAR T Consortium. *J Clin Oncol*. 2020;38(27):3119-3128.

36. Tibshirani RJ, Taylor J, Lockhart R, Tibshirani R. Exact post-selection inference for sequential regression procedures. *J Am Stat Assoc*. 2016;111(514):600-620.

37. Davis JE, Sharpe C, Mason K, Tam CS, Koldej RM, Ritchie DS. Ibrutinib protects T cells in patients with CLL from proliferation-induced senescence. *J Transl Med*. 2021;19(1):473.

38. Li J, Zhang Y, Yang C, Rong R. Discrepant mRNA and protein expression in immune cells. *Curr Genomics*. 2020;21(8):560-563.

39. Hamilton MP, Miklos DB. Chimeric antigen receptor T-cell therapy in aggressive B-cell lymphoma. *Hematol Oncol Clin North Am*. 2023;37(6):1053-1075.

40. Locke FL, Rossi JM, Neelapu SS, et al. Tumor burden, inflammation, and product attributes determine outcomes of axicabtagene ciloleucel in large B-cell lymphoma. *Blood Adv*. 2020;4(19):4898-4911.

41. Blumenberg V, Galina B, Baumann S, et al. Early quantification of anti-CD19 CAR T-cells by flow cytometry predicts response in R/R DLBCL. *Blood Adv*. 2023;7(22):6844-6849.

42. Dai Q, Han P, Qi X, et al. 4-1BB signaling boosts the anti-tumor activity of CD28-incorporated 2(nd) generation chimeric antigen receptor-modified T cells. *Front Immunol*. 2020;11:539654.

43. Smith R, Shen R. Complexities in comparing the impact of costimulatory domains on approved CD19 CAR functionality. *J Transl Med*. 2023;21(1):515.

44. Neelapu SS, Dickinson M, Munoz J, et al. Axicabtagene ciloleucel as first-line therapy in high-risk large B-cell lymphoma: the phase 2 ZUMA-12 trial. *Nat Med*. 2022;28(4):735-742.

45. Filosto S, Vardhanabhuti S, Canales MA, et al. Product attributes of CAR T-cell therapy differentially associate with efficacy and toxicity in second-line large B-cell lymphoma (ZUMA-7). *Blood Cancer Discov*. 2024;5(1):21-33.